Field Line Resonance in Two and a Half Dimensions

Charles McEachern

Advisor: Bob Lysak

Earth's Magnetic Field

When shaken by the solar wind, etc, Earth's dipole field rattles.

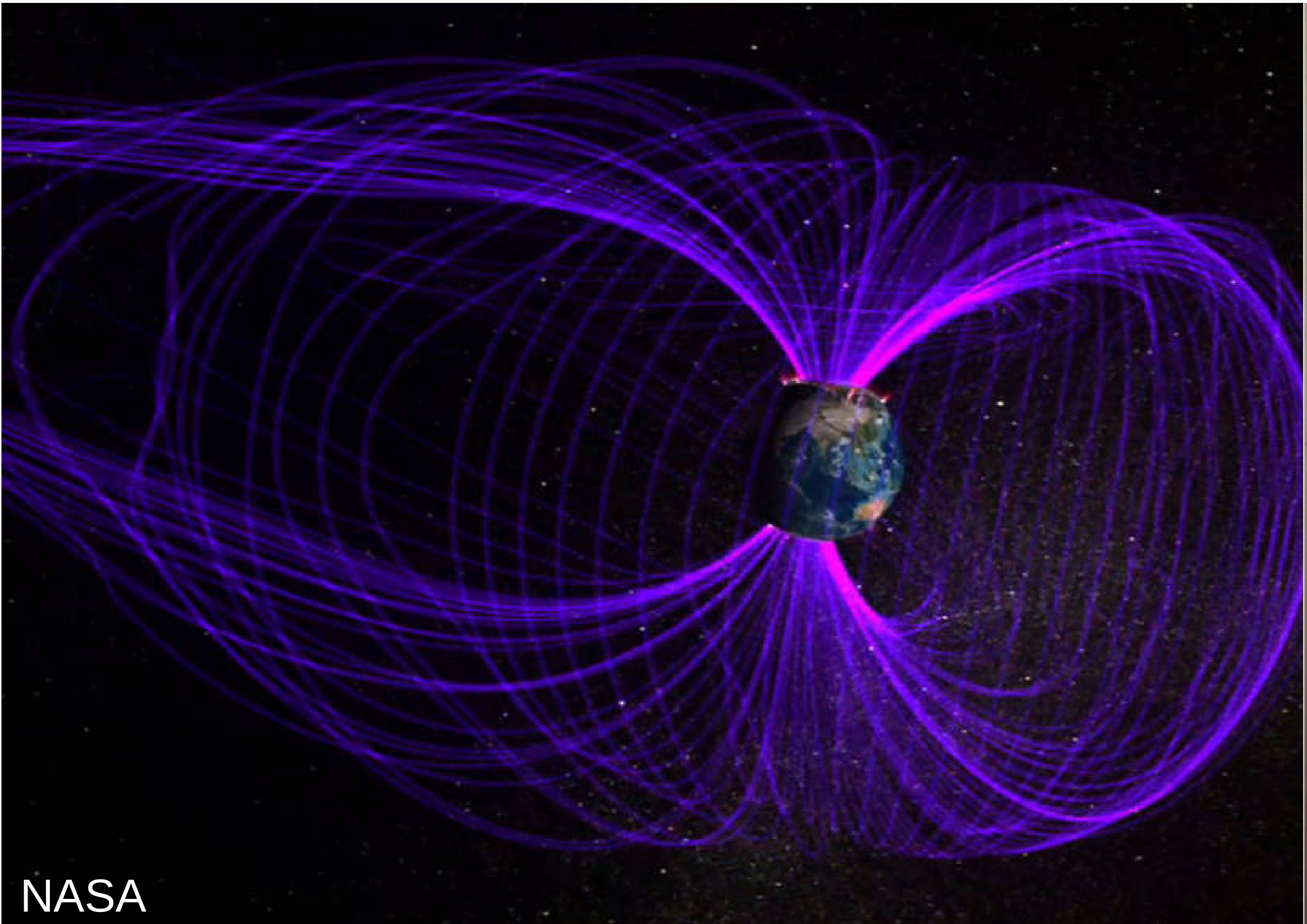
NASA


Flóra Borsi

Particles in a Dipole Field

- Three fundamental motions: gyro, bounce, drift.
- Resonance happens when particle frequency matches wave frequency.

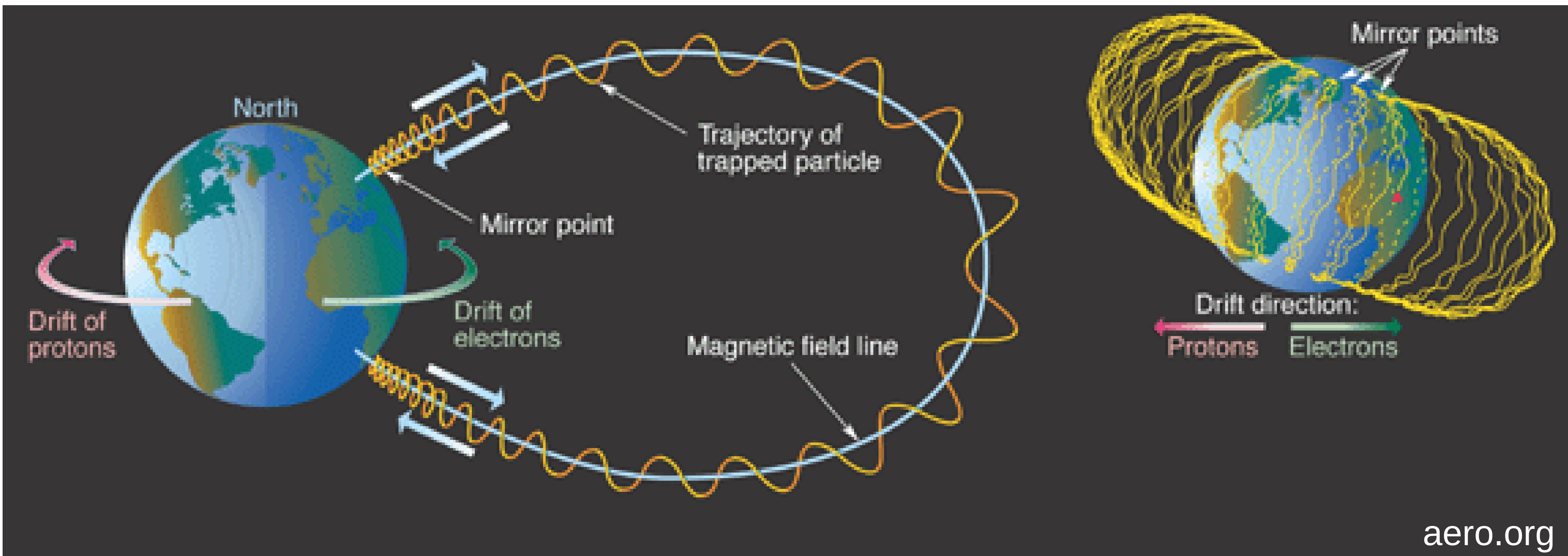

Alfvén Waves

- Shear Alfvén waves carry energy along the magnetic field.
- Compressional Alfvén waves can carry energy across field lines.

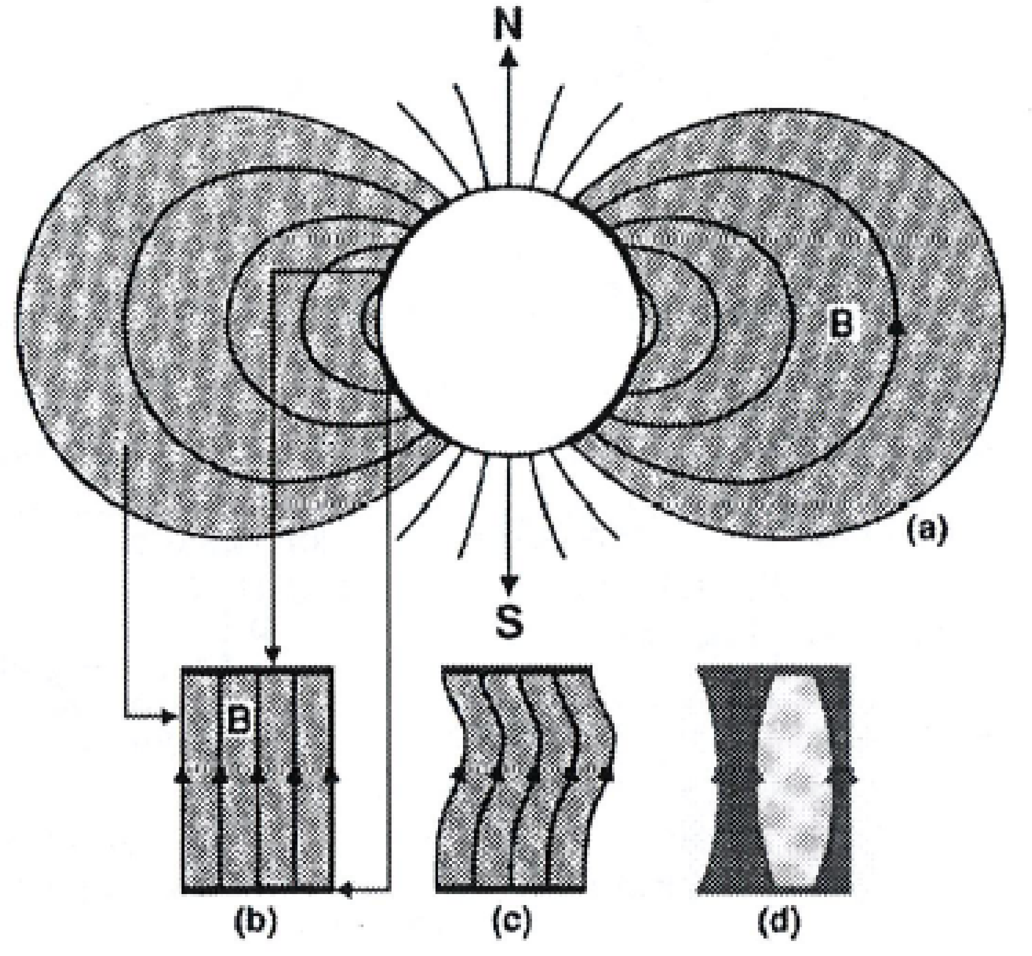

Odd and Even Harmonics

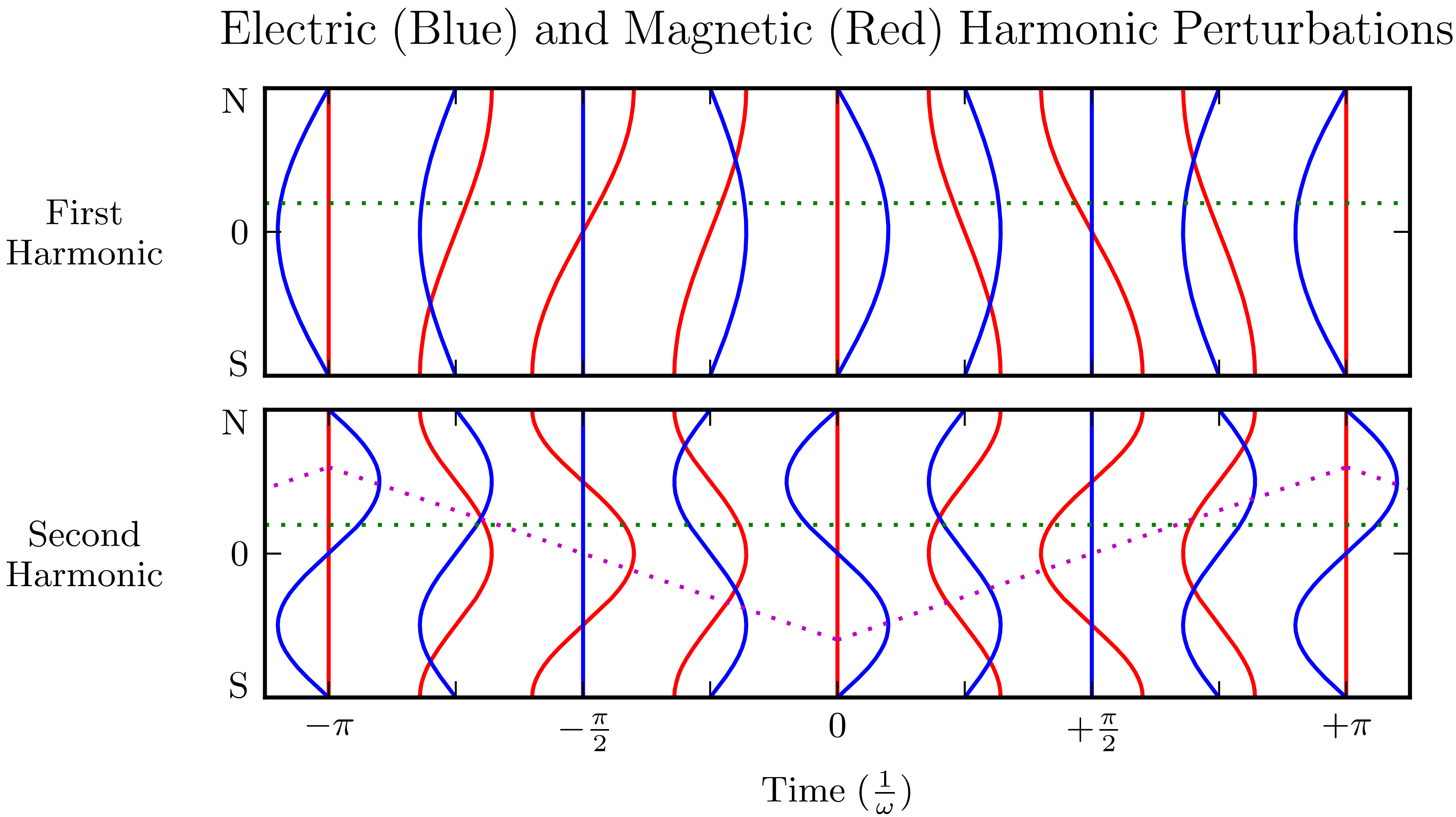

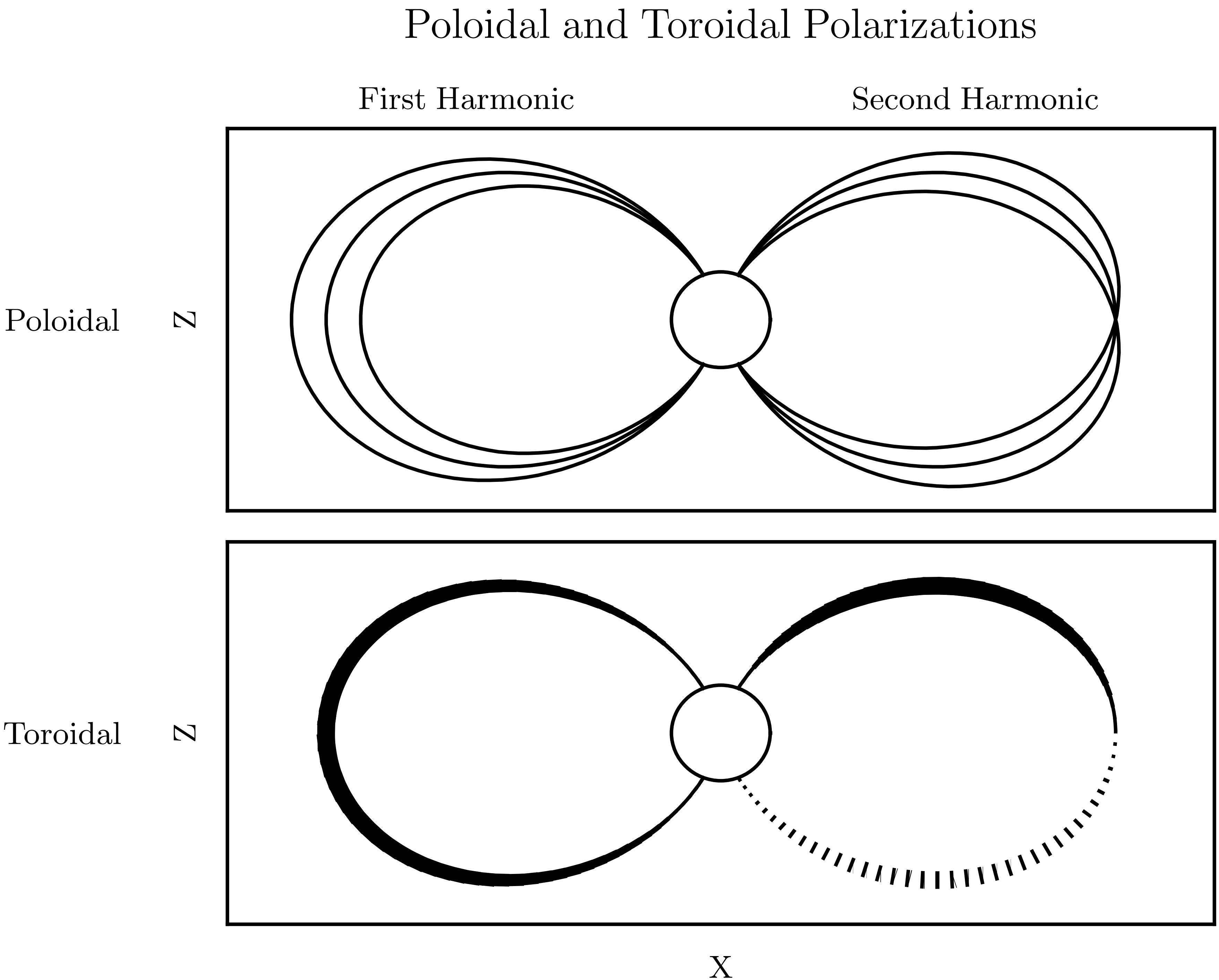

Poloidal and Toroidal Polarizations
First Harmonic
Second Harmonic
Poloidal
Z
Toroidal
Z
X

Azimuthal Modenumber

- Small *m* waves tend to be driven externally.
- Large *m* waves are driven internally.

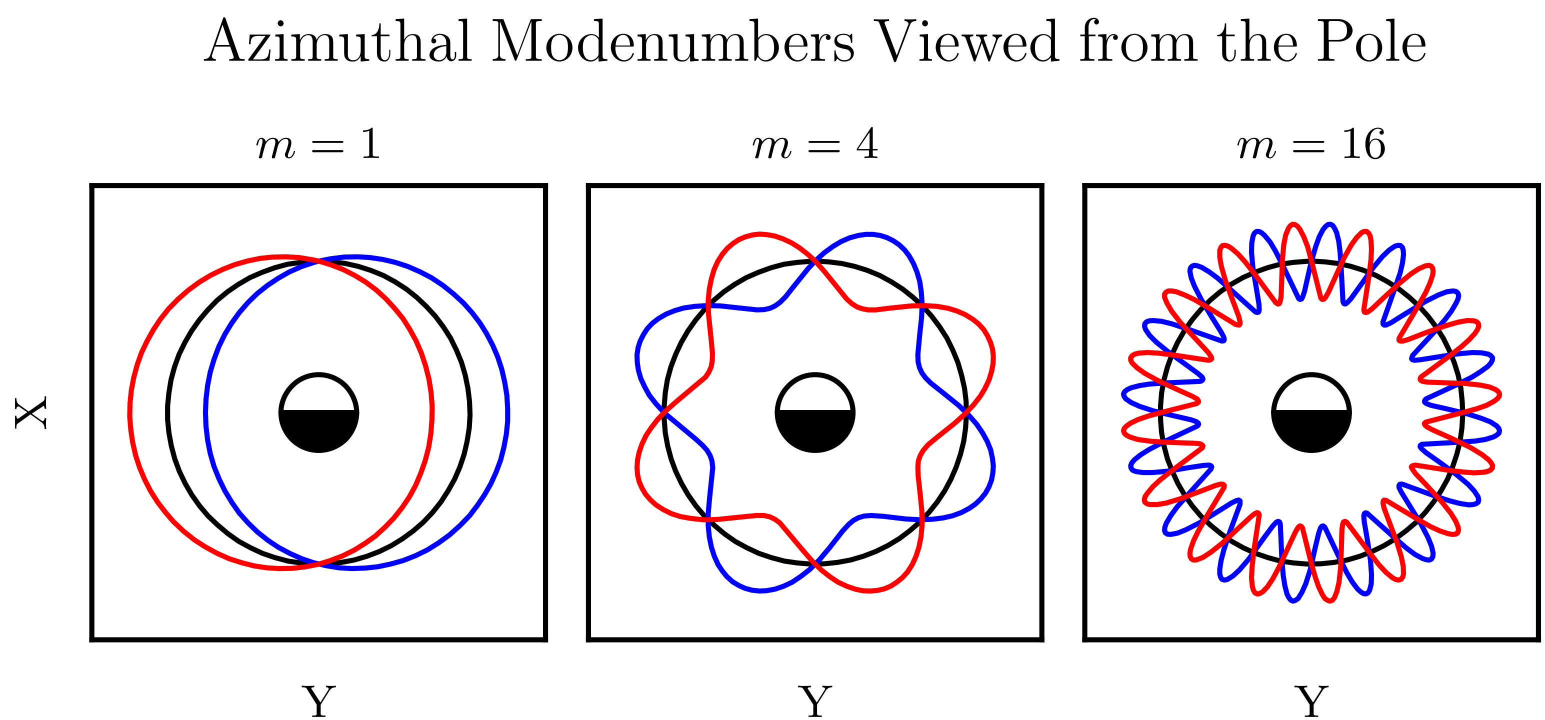

Pc4s and Giant Pulsations

Pc4s:

- FLR at 7mHz to 25mHz.
- Mostly toroidal.
- Peak near noon.

Pg:

- Odd poloidal Pc4.
- Peak near midnight.
- Striking ground signature.
- Typically 16 < m < 35.

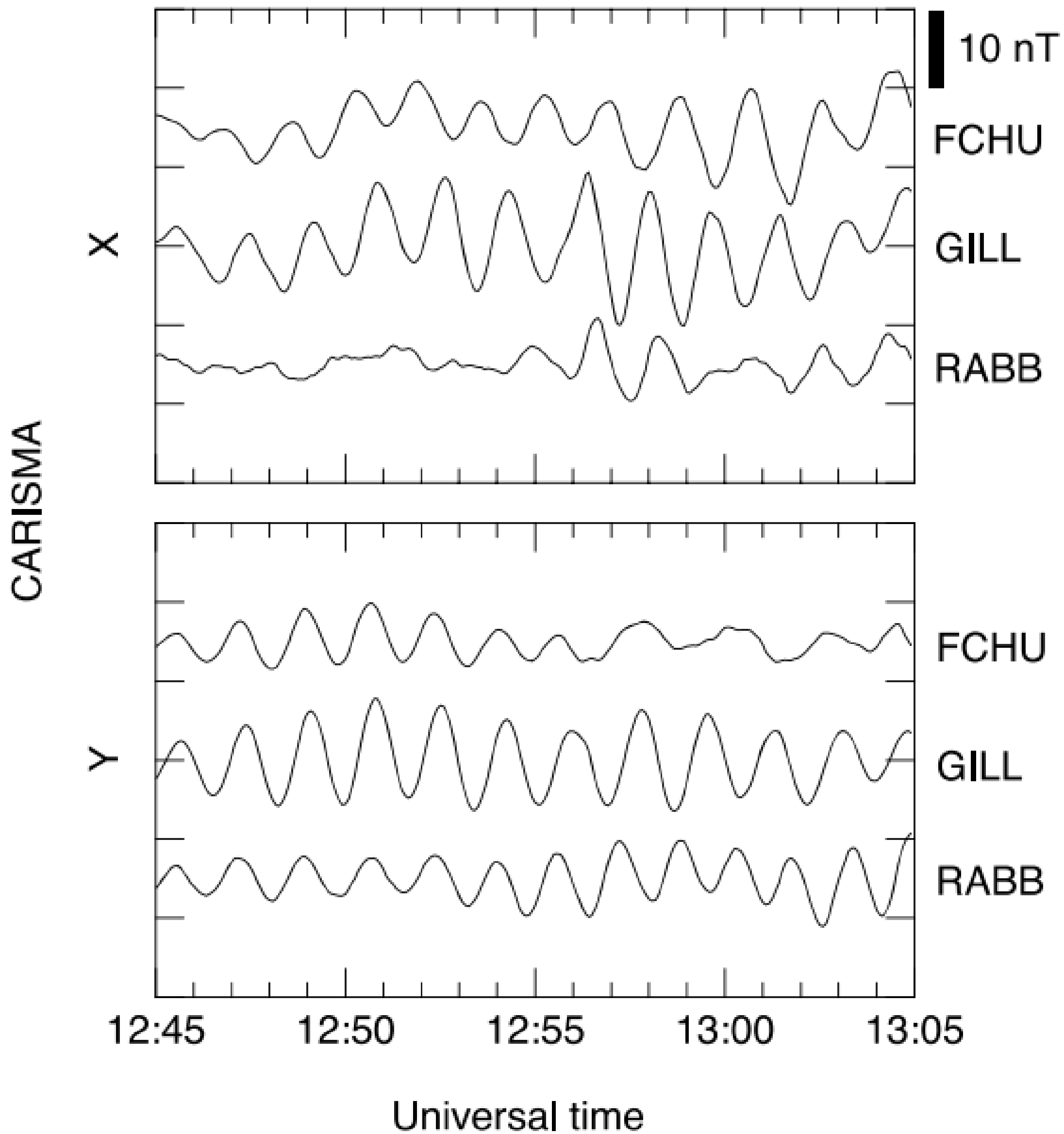

Takahashi, 2011

Outline

- Intro (done!)
- Numerical Model
- Numerical Results
- Van Allen Probe Observations

“Tuna Half” Dimensions

- The ionosphere is important to FLRs, but is also computationally demanding.
- High-*m* waves are of particular interest, but are hard to resolve in 3D.
- We don't actually need to look at the dayside and nightside at the same time.
- Say everything goes as exp($im\varphi$).

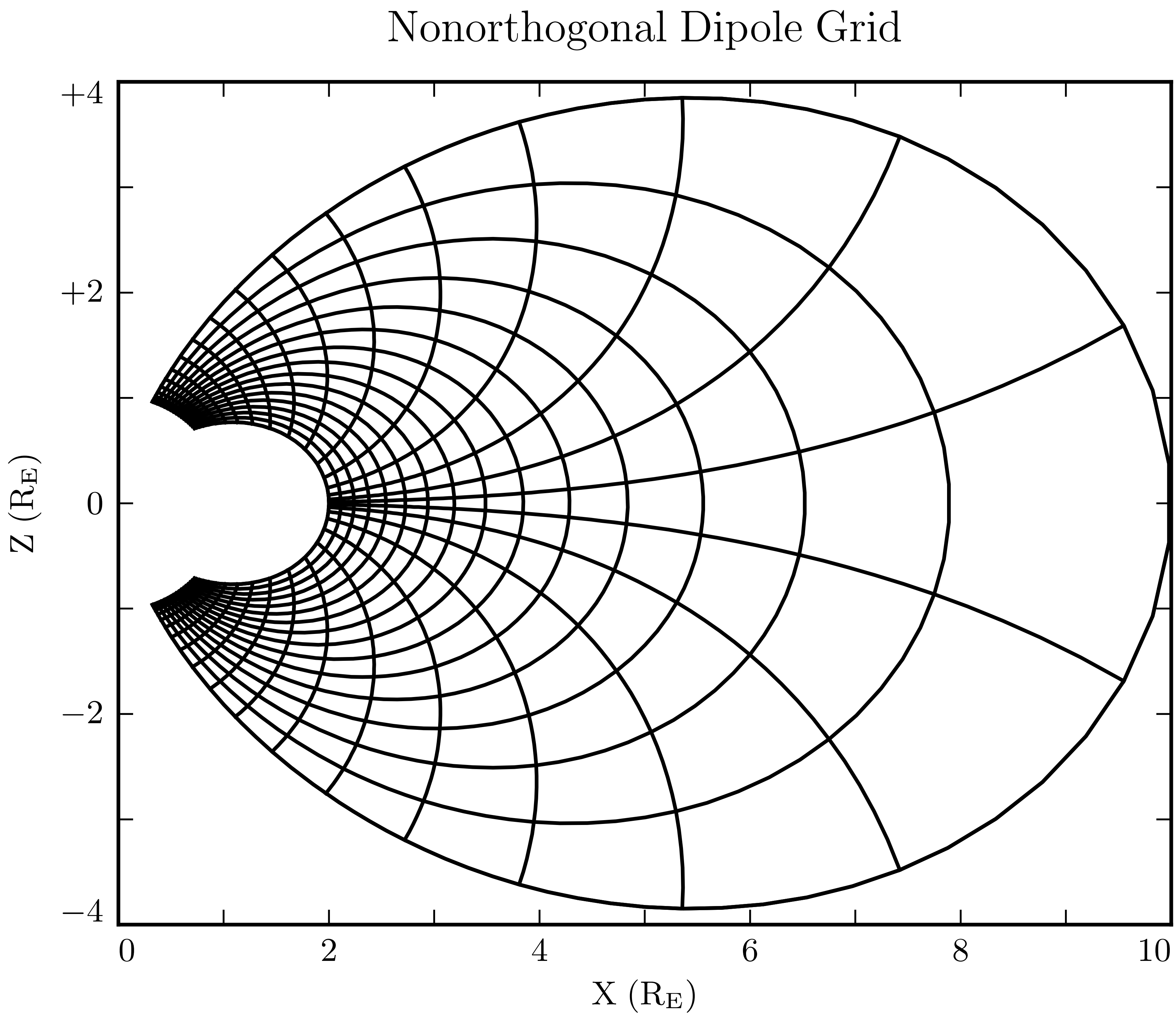
Nonorthogonal Dipole Grid
+4
+2
0
−2
−4
Z (R$_E$)
0
2
4
6
8
10
X (R$_E$)

Physical Parameter Profiles

- Background dipole magnetic field.
- Height-resolved conductivity profiles.
- Density profile, including the plasmasphere.
- Alfvén speed.

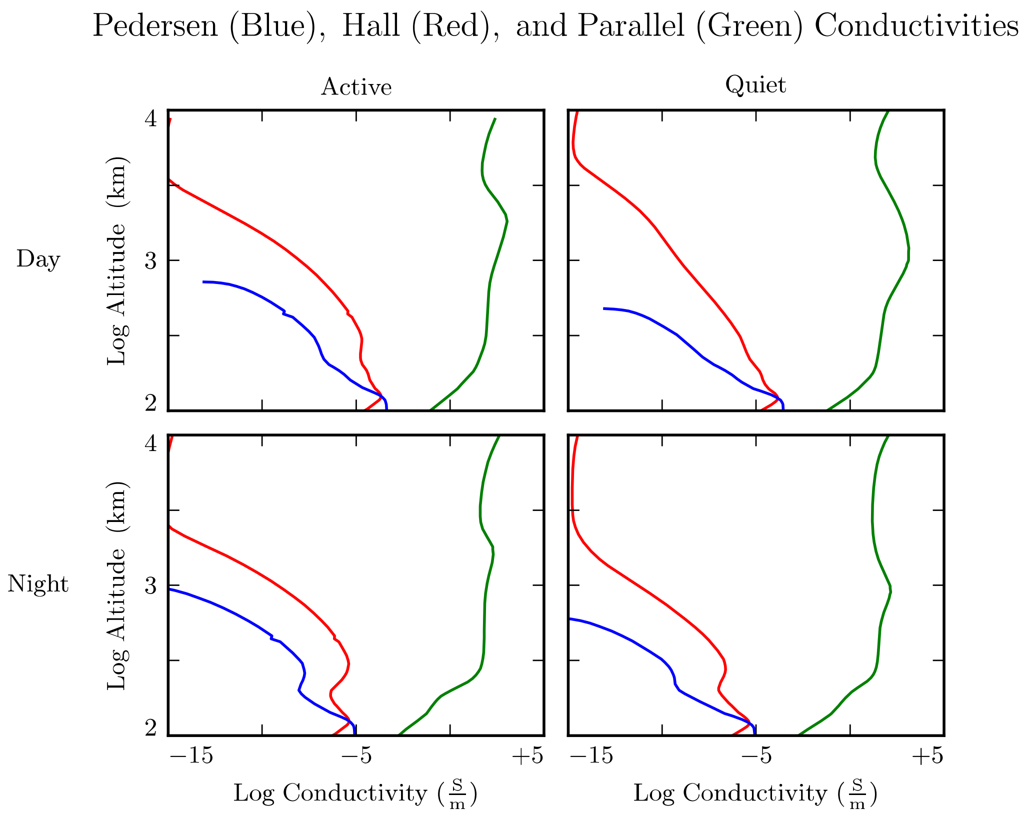

Driving with Compression?

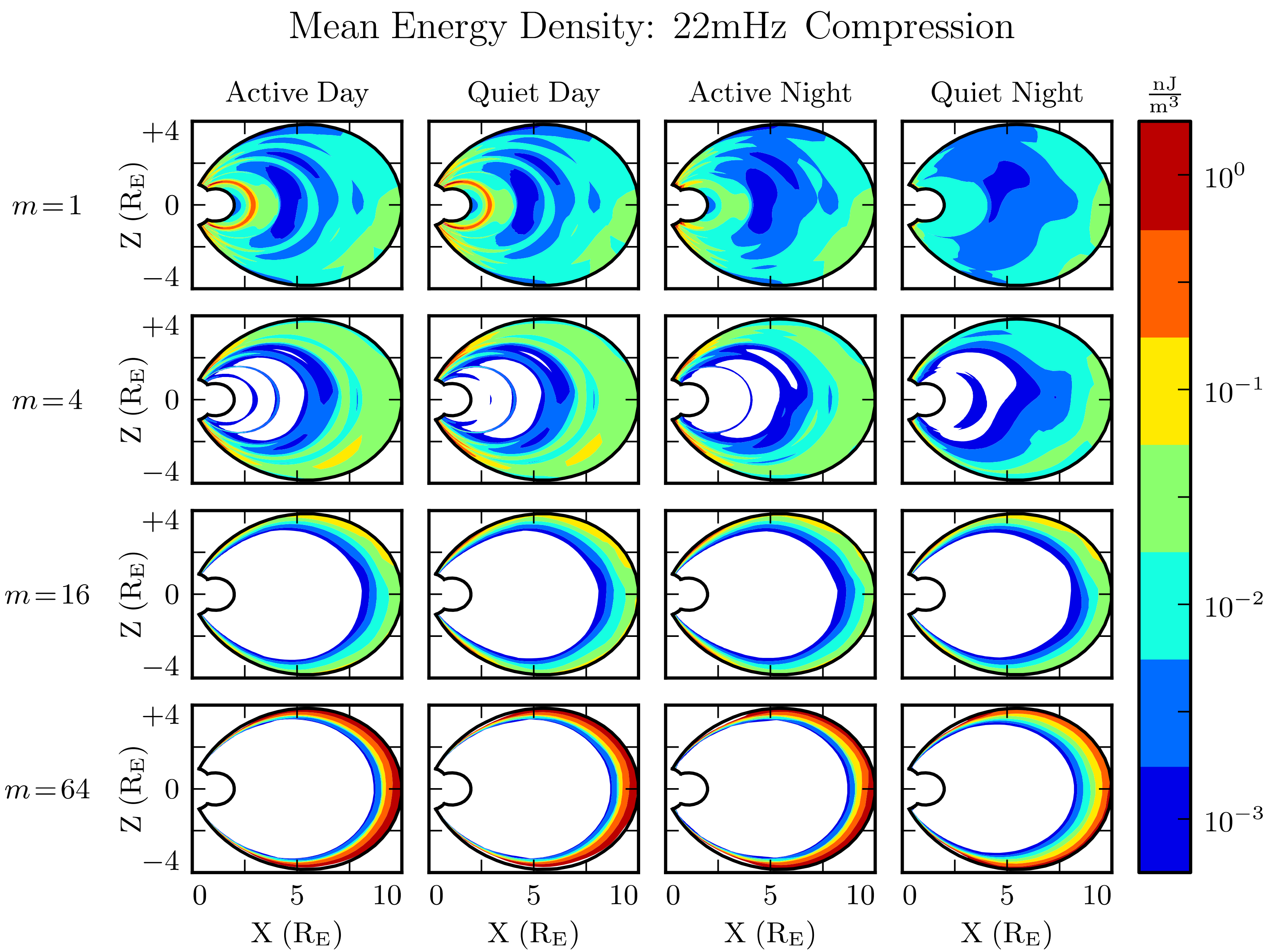

Driving with Current

- From Sym-H pink noise, estimate the strength of ring current perturbations at 10 mHz.

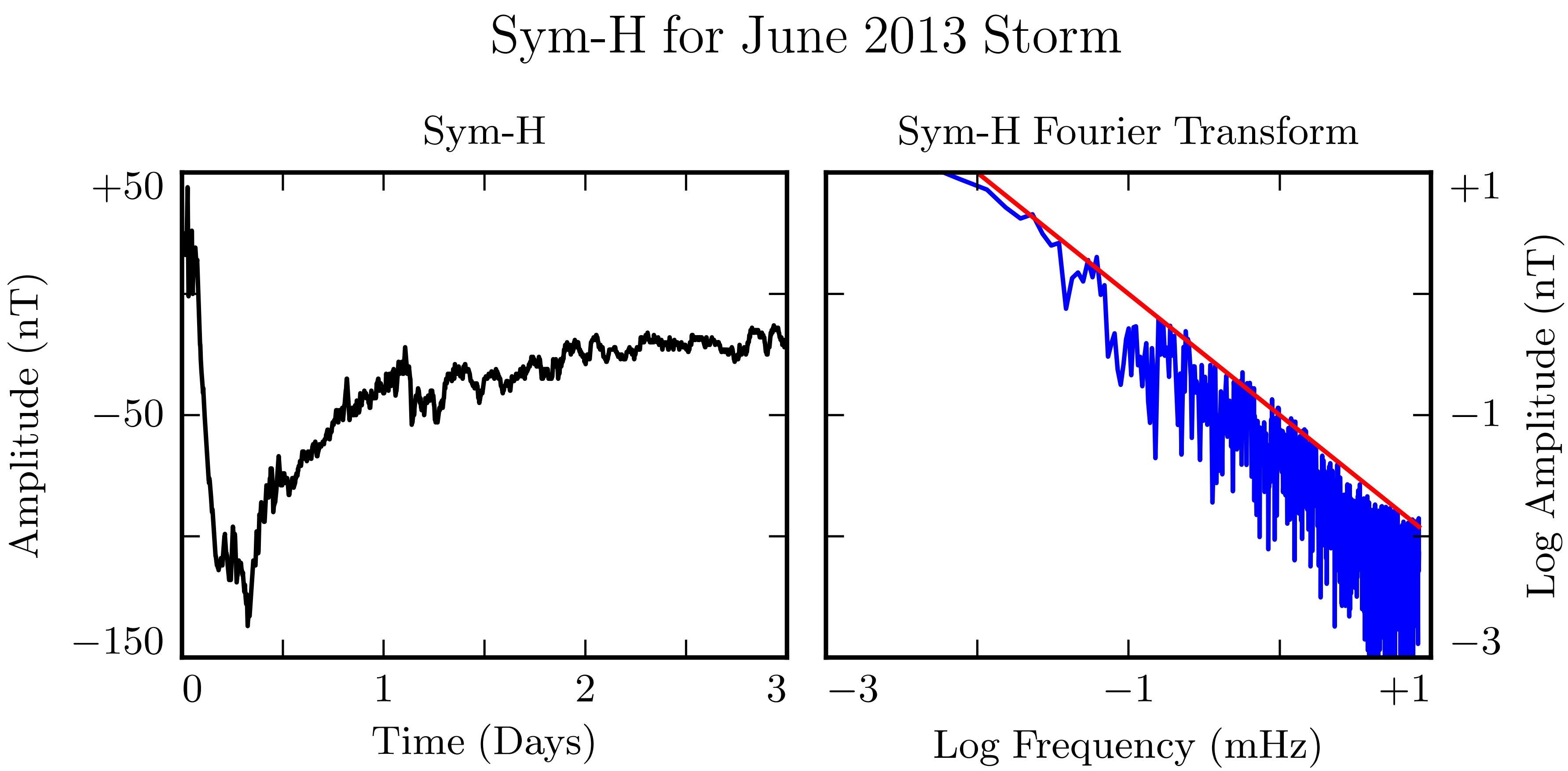

Maxwell's Equations

$$\frac{\partial}{\partial t}\underline{B} = -\nabla \times \underline{E}$$

$$\underline{C} \equiv \nabla \times \underline{E}$$

$$B_1 \leftarrow B_1 - g_{11}\,\delta t\,C^1 - g_{13}\,\delta t\,C^3$$

$$B_2 \leftarrow B_2 - g_{22}\,\delta t\,C^2$$

$$B_3 \leftarrow B_3 - g_{31}\,\delta t\,C^1 - g_{33}\,\delta t\,C^3$$

$$\underline{\underline{\epsilon}} \cdot \frac{\partial}{\partial t}\underline{E} = \frac{1}{\mu_0}\nabla \times \underline{B} - \underline{J} - \underline{\underline{\sigma}} \cdot \underline{E}$$

$$\underline{F} \equiv \nabla \times \underline{B} - \mu_0 \underline{J}$$

$$\left(\underline{\underline{\Omega}} + \underline{\underline{\mathbb{I}}}\frac{\partial}{\partial t}\right) \cdot \underline{E} = \underline{\underline{V}}^2 \cdot \underline{F}$$

$$\underline{\underline{V}}^2 \equiv \frac{1}{\mu_0}\underline{\underline{\epsilon}}^{-1} \quad \text{and} \quad \underline{\underline{\Omega}} \equiv \underline{\underline{\epsilon}}^{-1} \cdot \underline{\underline{\sigma}}$$

$$\begin{aligned} E_1 + \frac{g^{13}}{g^{11}}E_3 \leftarrow\ & E_1 \cos\left(\tfrac{-\sigma_H \delta t}{\epsilon_\perp}\right) \exp\left(\tfrac{-\sigma_P \delta t}{\epsilon_\perp}\right) \\ & + E_2 \sin\left(\tfrac{-\sigma_H \delta t}{\epsilon_\perp}\right) \exp\left(\tfrac{-\sigma_P \delta t}{\epsilon_\perp}\right) \sqrt{\frac{g^{22}}{g^{11}}} \\ & + E_3 \cos\left(\tfrac{-\sigma_H \delta t}{\epsilon_\perp}\right) \exp\left(\tfrac{-\sigma_P \delta t}{\epsilon_\perp}\right) \frac{g^{13}}{g^{11}} \\ & + F^1 \cos\left(\tfrac{-\sigma_H \delta t}{2\epsilon_\perp}\right) \exp\left(\tfrac{-\sigma_P \delta t}{2\epsilon_\perp}\right) \frac{v_A^2 \delta t}{g^{11}} \\ & + F^2 \sin\left(\tfrac{-\sigma_H \delta t}{2\epsilon_\perp}\right) \exp\left(\tfrac{-\sigma_P \delta t}{2\epsilon_\perp}\right) \frac{v_A^2 \delta t}{\sqrt{g^{11} g^{22}}} \end{aligned}$$

$$\begin{aligned} E_2 \leftarrow & -E_1 \sin\left(\tfrac{-\sigma_H \delta t}{\epsilon_\perp}\right) \exp\left(\tfrac{-\sigma_P \delta t}{\epsilon_\perp}\right) \sqrt{\frac{g^{11}}{g^{22}}} \\ & + E_2 \cos\left(\tfrac{-\sigma_H \delta t}{\epsilon_\perp}\right) \exp\left(\tfrac{-\sigma_P \delta t}{\epsilon_\perp}\right) \\ & - E_3 \sin\left(\tfrac{-\sigma_H \delta t}{\epsilon_\perp}\right) \exp\left(\tfrac{-\sigma_P \delta t}{\epsilon_\perp}\right) \frac{g^{13}}{\sqrt{g^{11} g^{22}}} \\ & - F^1 \sin\left(\tfrac{-\sigma_H \delta t}{2\epsilon_\perp}\right) \exp\left(\tfrac{-\sigma_P \delta t}{2\epsilon_\perp}\right) \frac{v_A^2 \delta t}{\sqrt{g^{11} g^{22}}} \\ & + F^2 \cos\left(\tfrac{-\sigma_H \delta t}{2\epsilon_\perp}\right) \exp\left(\tfrac{-\sigma_P \delta t}{2\epsilon_\perp}\right) \frac{v_A^2 \delta t}{g^{22}} \end{aligned}$$

$$E_3 \leftarrow E_3 \exp\left(\tfrac{-\sigma_0 \delta t}{\epsilon_0}\right) + c^2 \delta t \left(g_{31} F^1 + g_{33} F^3\right) \exp\left(\tfrac{-\sigma_0 \delta t}{2\epsilon_0}\right)$$

Electron Inertial Effects

$$0 = \sigma_0 E_z - J_z \qquad \text{becomes} \qquad \frac{1}{\nu}\frac{\partial}{\partial t} J_z = \sigma_0 E_z - J_z$$

Parallel Electric Fields: Quiet Day, 100s of 16mHz Current, $m = 16$

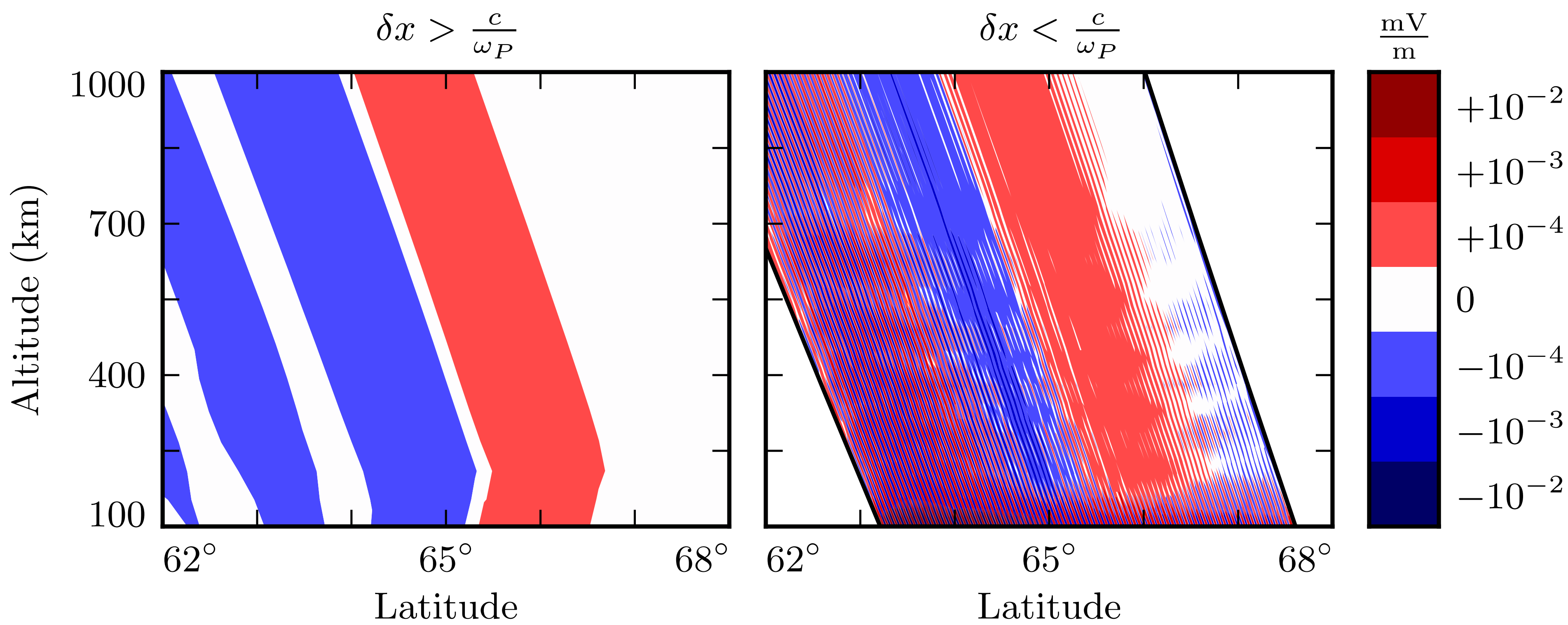

Coupling to the Atmosphere

$\nabla \times \underline{B} = 0$ and $\nabla \cdot \underline{B} = 0$

so $\underline{B} = \nabla\Psi$ where $\nabla^2\Psi = 0$

$$\underline{\underline{\Sigma}} \cdot \underline{E} = \frac{1}{\mu_0} \lim_{\delta r \to 0} \left[\hat{r} \times \underline{B} \right|_{R_I - \delta r}^{R_I + \delta r}$$

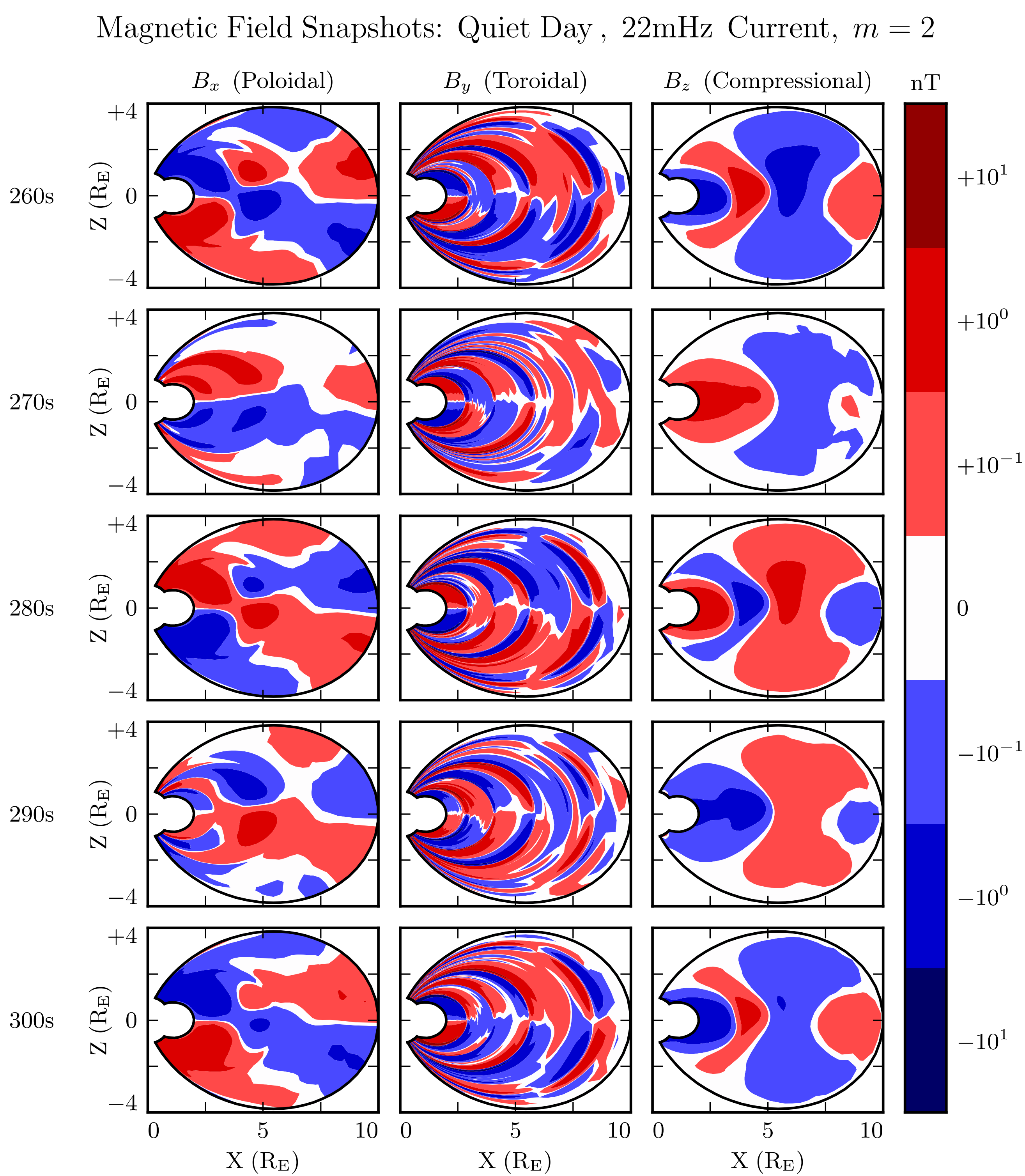

Magnetic Field Snapshots: Quiet Day, 22mHz Current, m = 2
Bx (Poloidal)
By (Toroidal)
Bz (Compressional)
nT
260s
270s
280s
290s
300s
Z (RE)
X (RE)
+4
0
−4
0
5
10
+10^1
+10^0
+10^−1
0
−10^−1
−10^0
−10^1

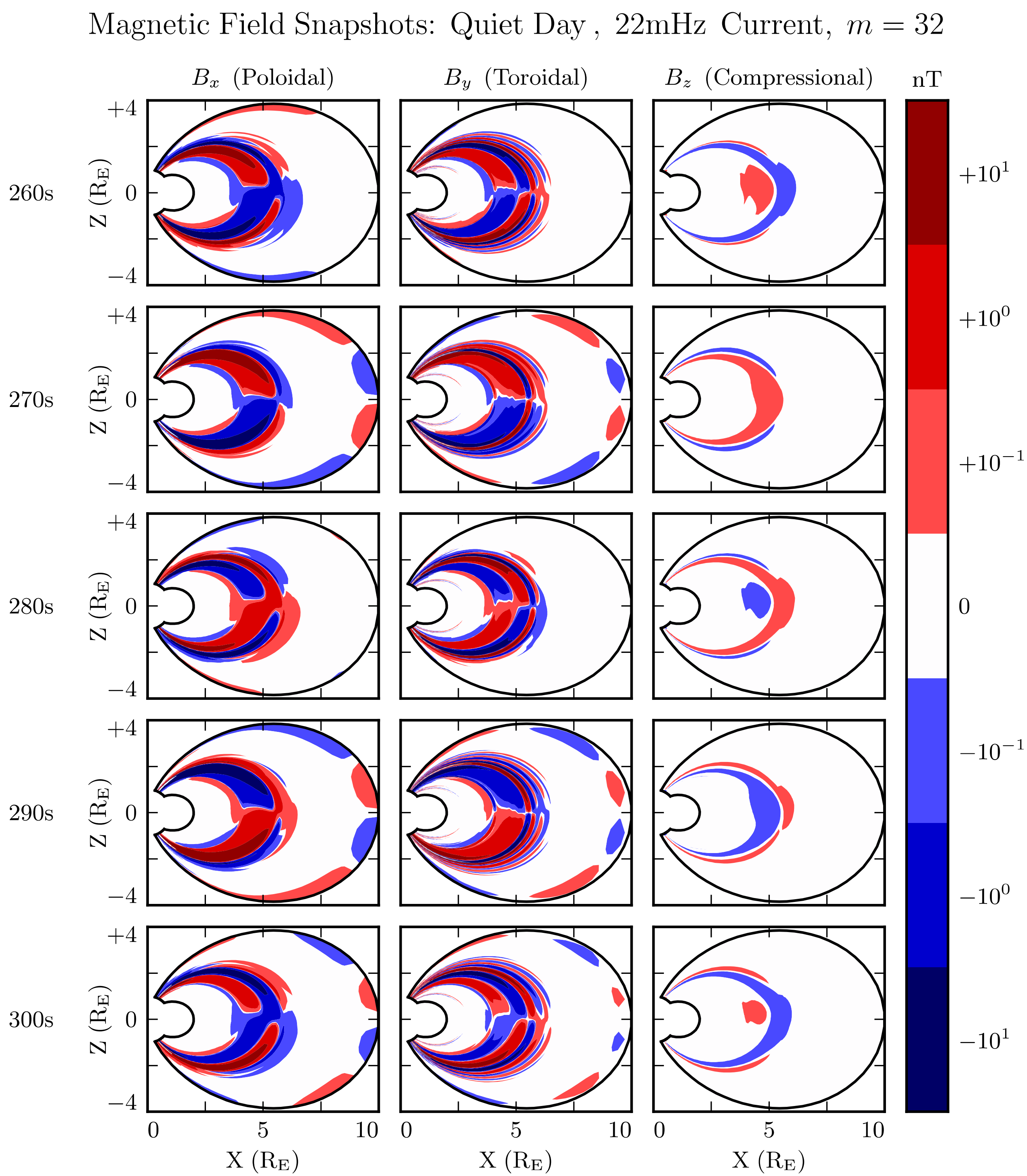

Magnetic Field Snapshots: Quiet Day , 22mHz Current, $m = 32$
B_x (Poloidal)
B_y (Toroidal)
B_z (Compressional)
nT
260s
270s
280s
290s
300s
Z (R_E)
X (R_E)
+4
0
−4
0
5
10
$+10^1$
$+10^0$
$+10^{-1}$
0
-10^{-1}
-10^0
-10^1

Poloidal-to-Toroidal Rotation

- Poloidal waves rotate to the toroidal mode over time.
- Low-*m* waves rotate faster.

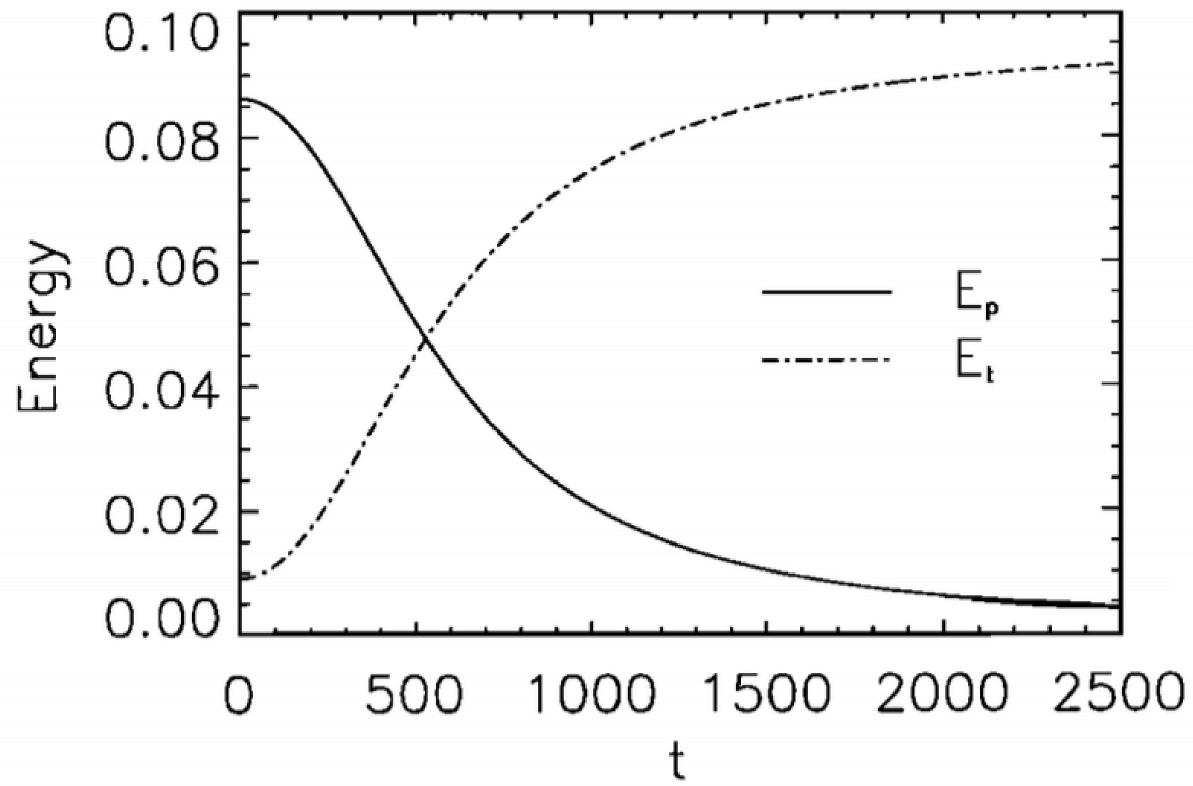

Figure 3. Time evolution of the $\hat{\mathbf{x}}$ integrated energy densities $E_p = \int_0^1 e_p \, dx$ and $E_t = \int_0^1 e_t \, dx$. The polarization rotation from poloidal to toroidal is clearly shown.

Mann and Wright, 1995

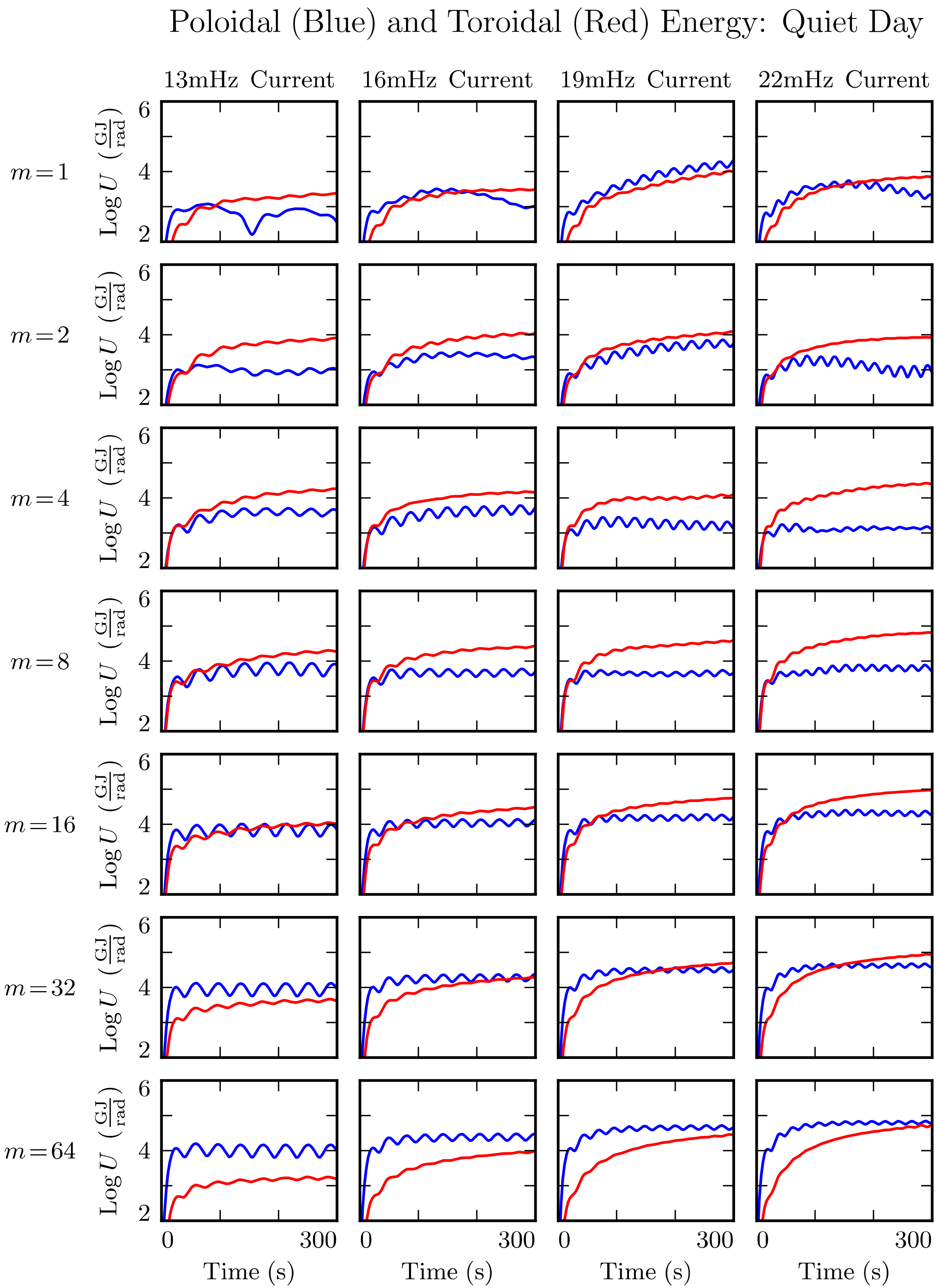

- Slowest rotation at high *m*.
- Faster rotation at moderate *m*.
- Low *m*: ???

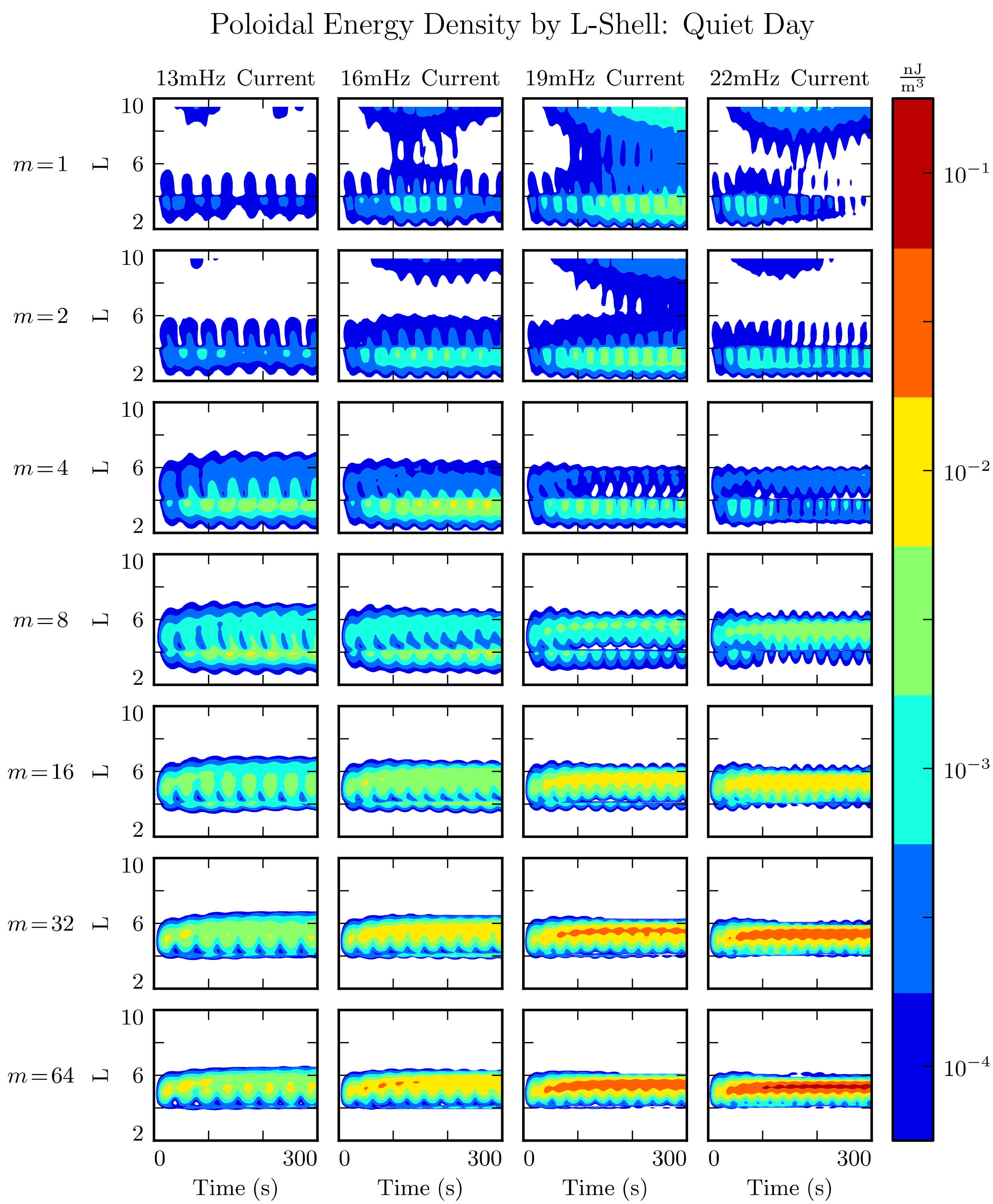

- Guided at high *m*.
- Escape at low *m*.
- Buildup near boundary likely nonphysical.

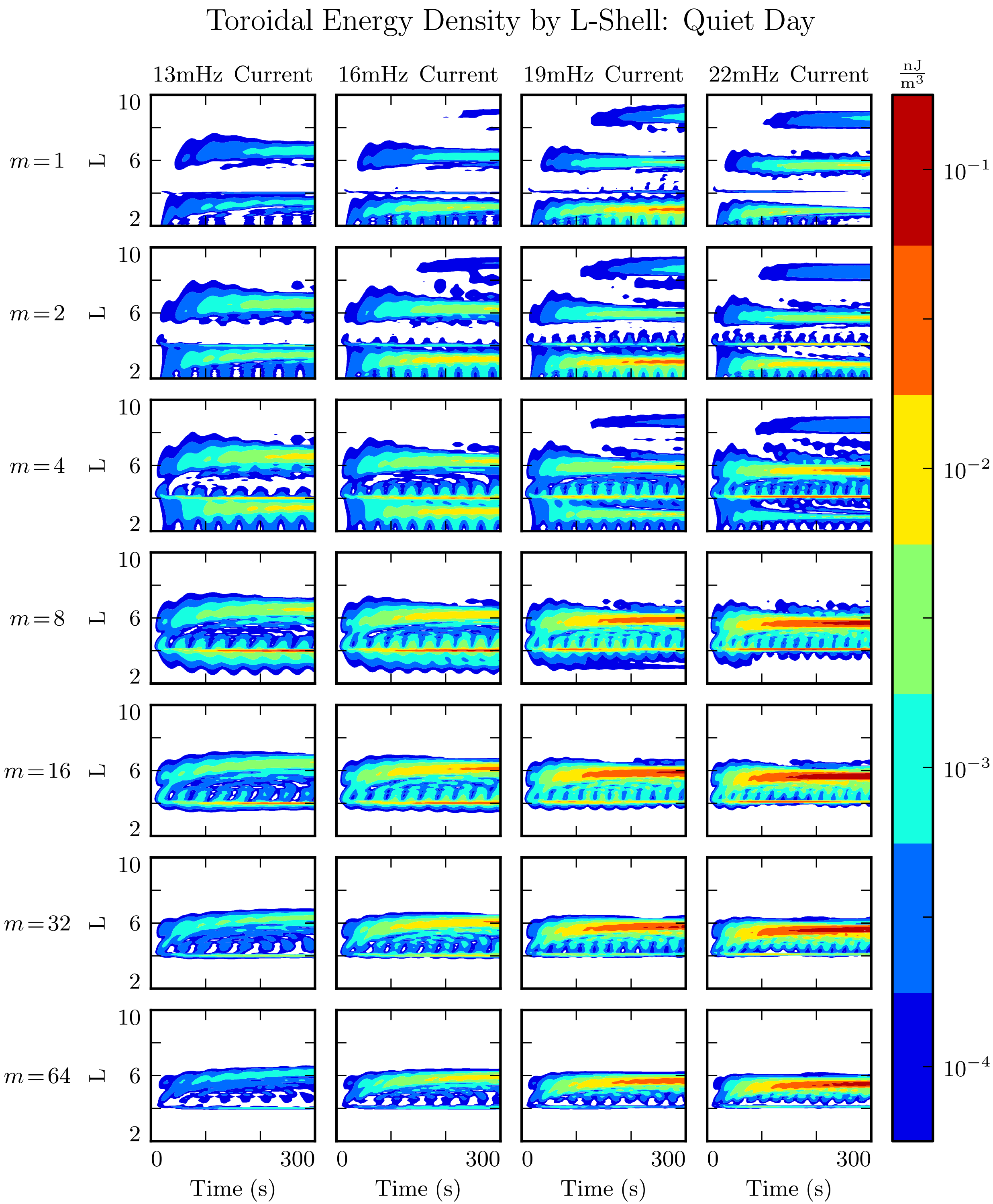

- Sharp in L, regardless of *m*.
- Asymptotically exceeds poloidal energy in most runs.

- Ionosphere is the only change.
- Low *m*: still weird.
- Moderate *m*: still best for toroidal.
- High *m*: toroidal very weak.

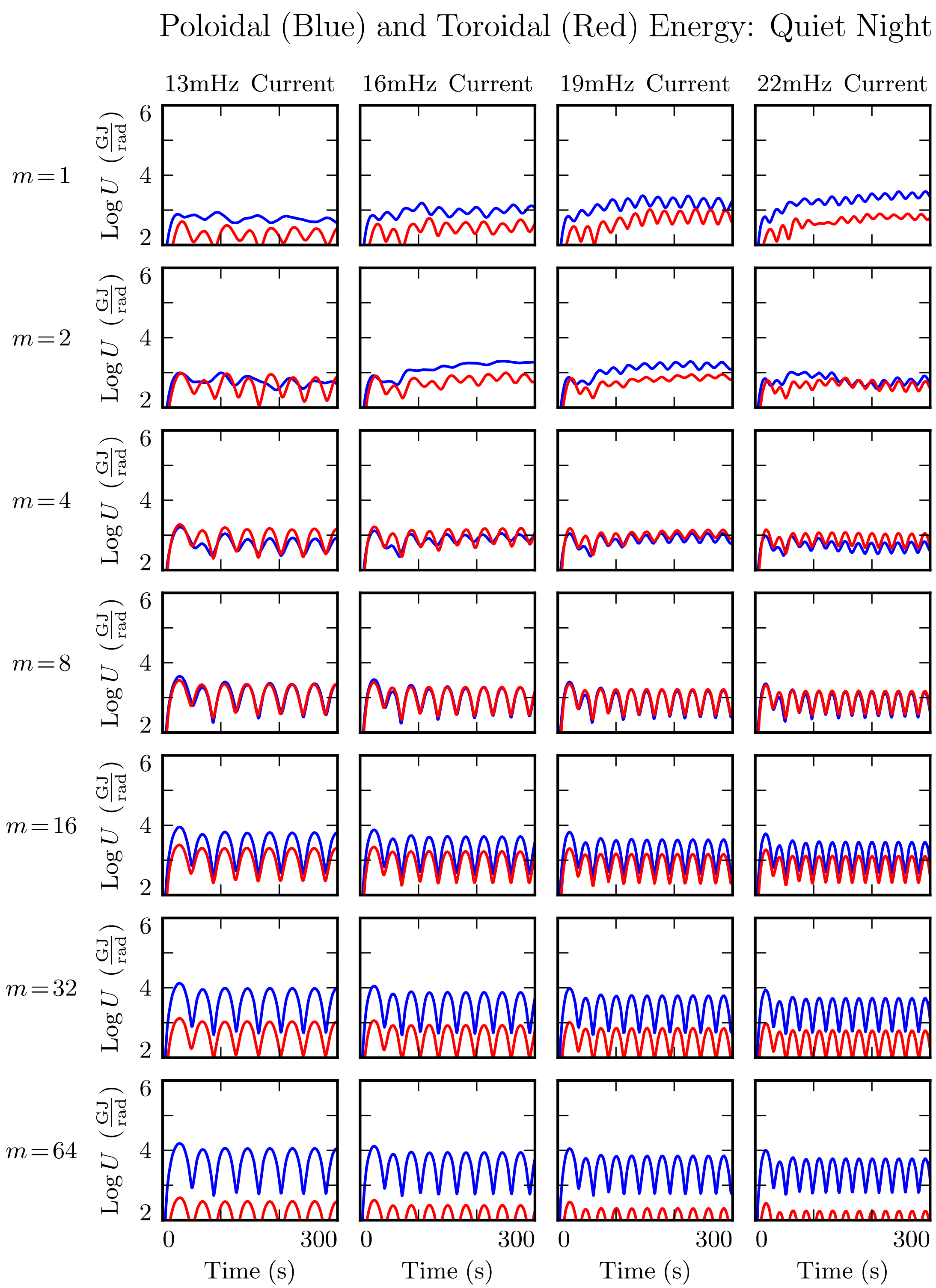

- Low *m*: still escaping.
- Higher *m* → more guided, stronger.
- Down 10x from the dayside.

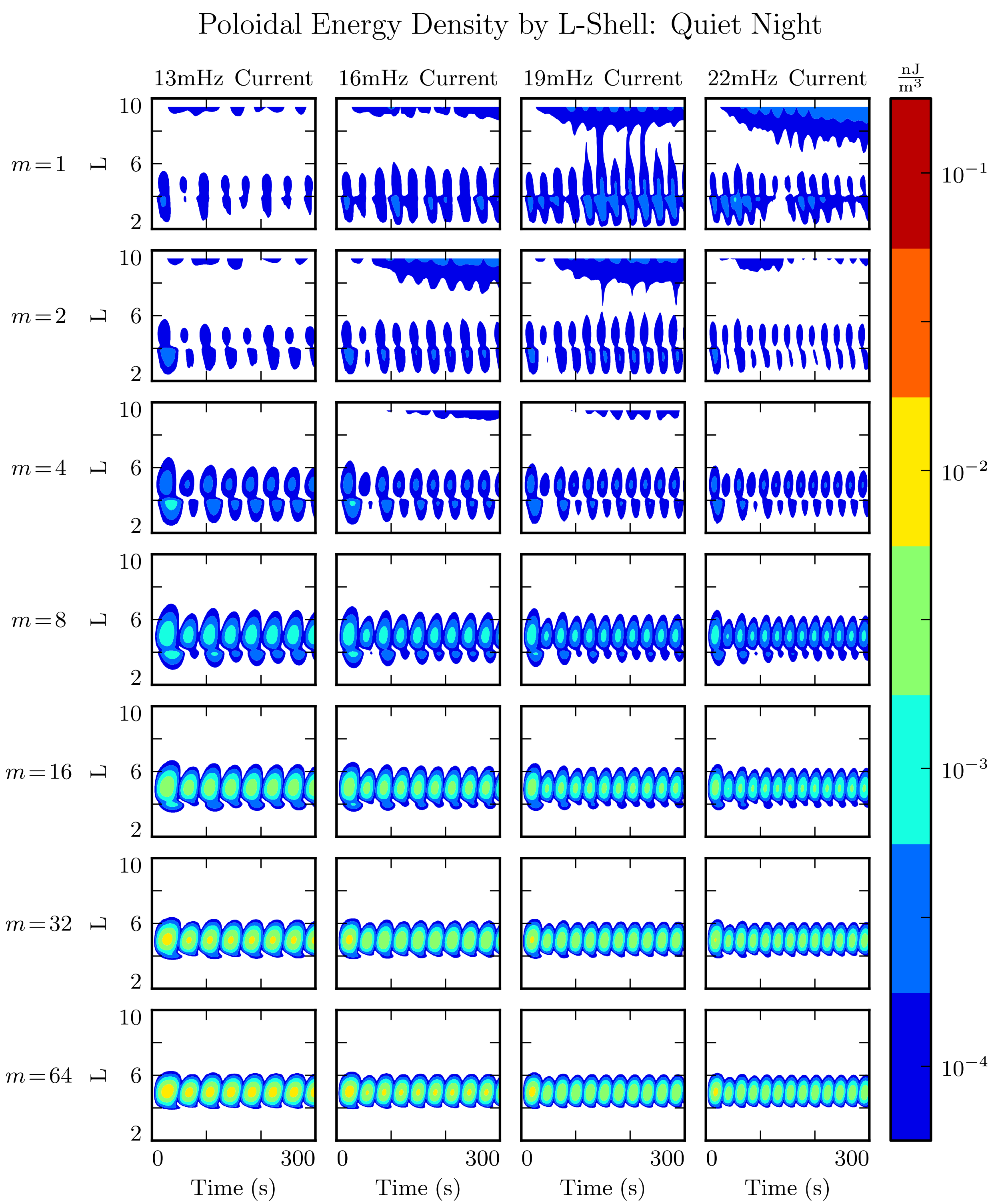

- Low to moderate *m*: weaker than dayside, but qualitatively similar.
- High *m*: barely exists. Rotation slower than Joule dissipation.

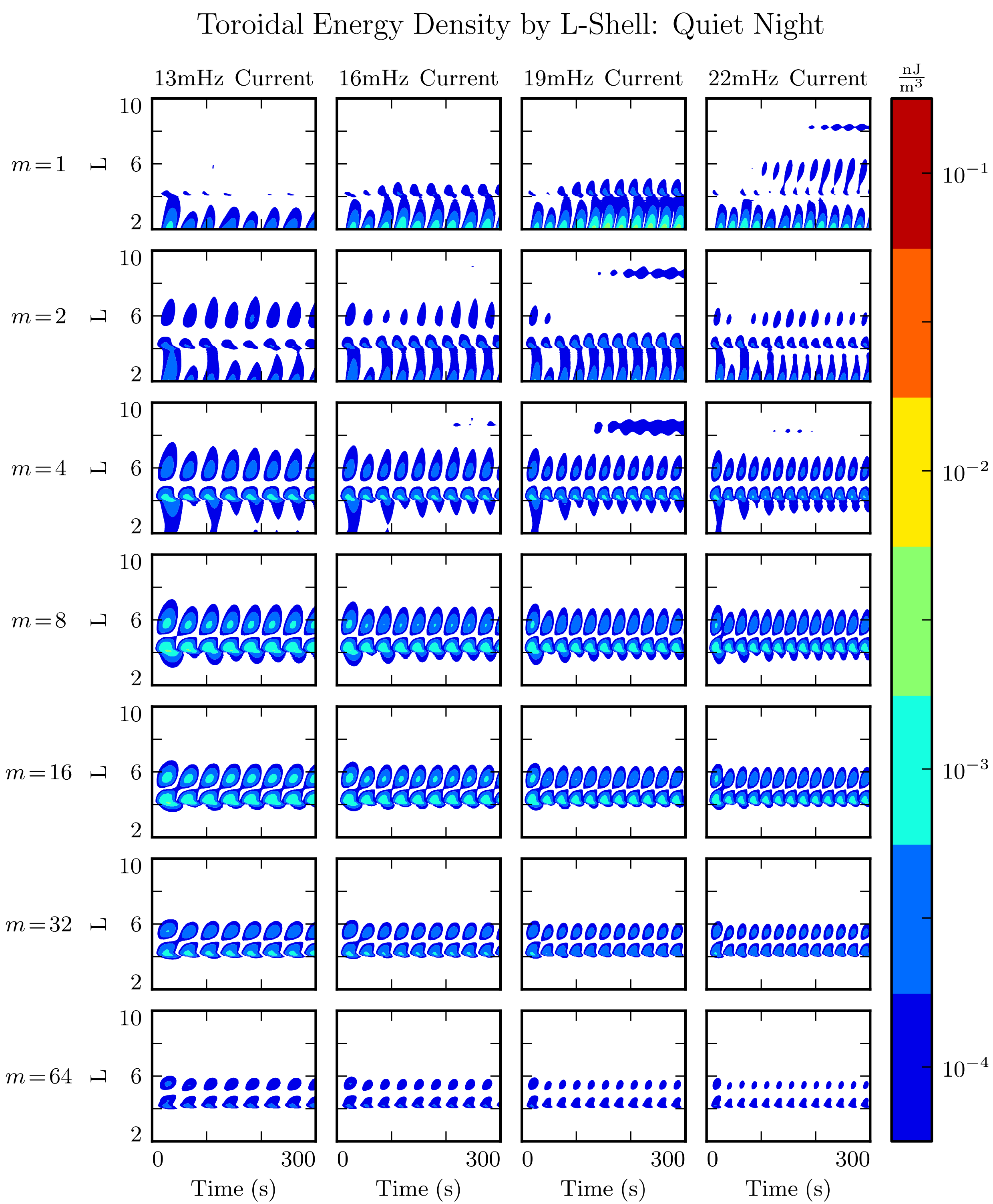

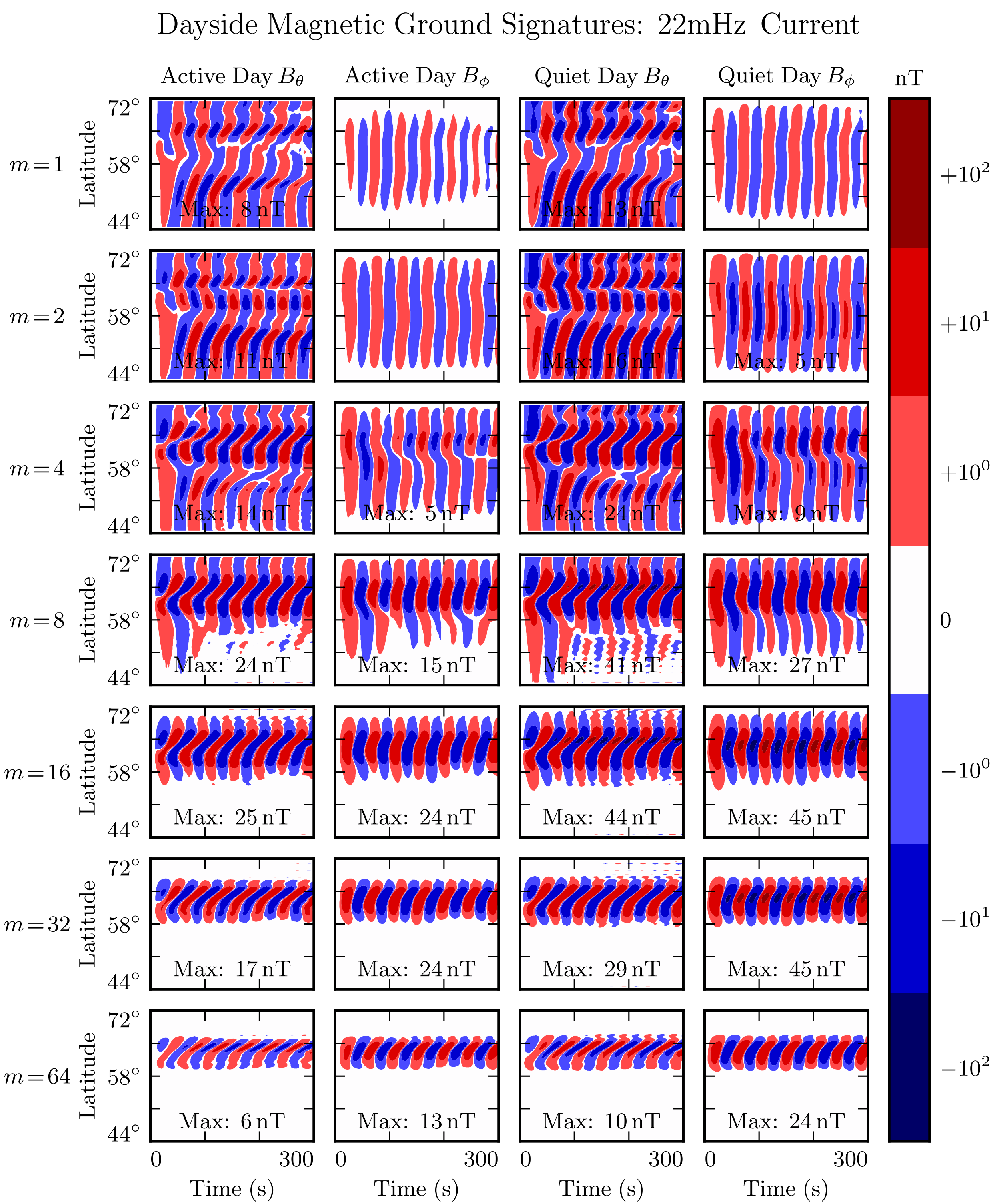

- Peak at *m*=16, 32.
- Mostly east-west polarized.
- Strongest for quiet profile.
- Low latitude CCW, high latitude CW.

- Weaker by a factor of 4.
- Pg properties still apparent.

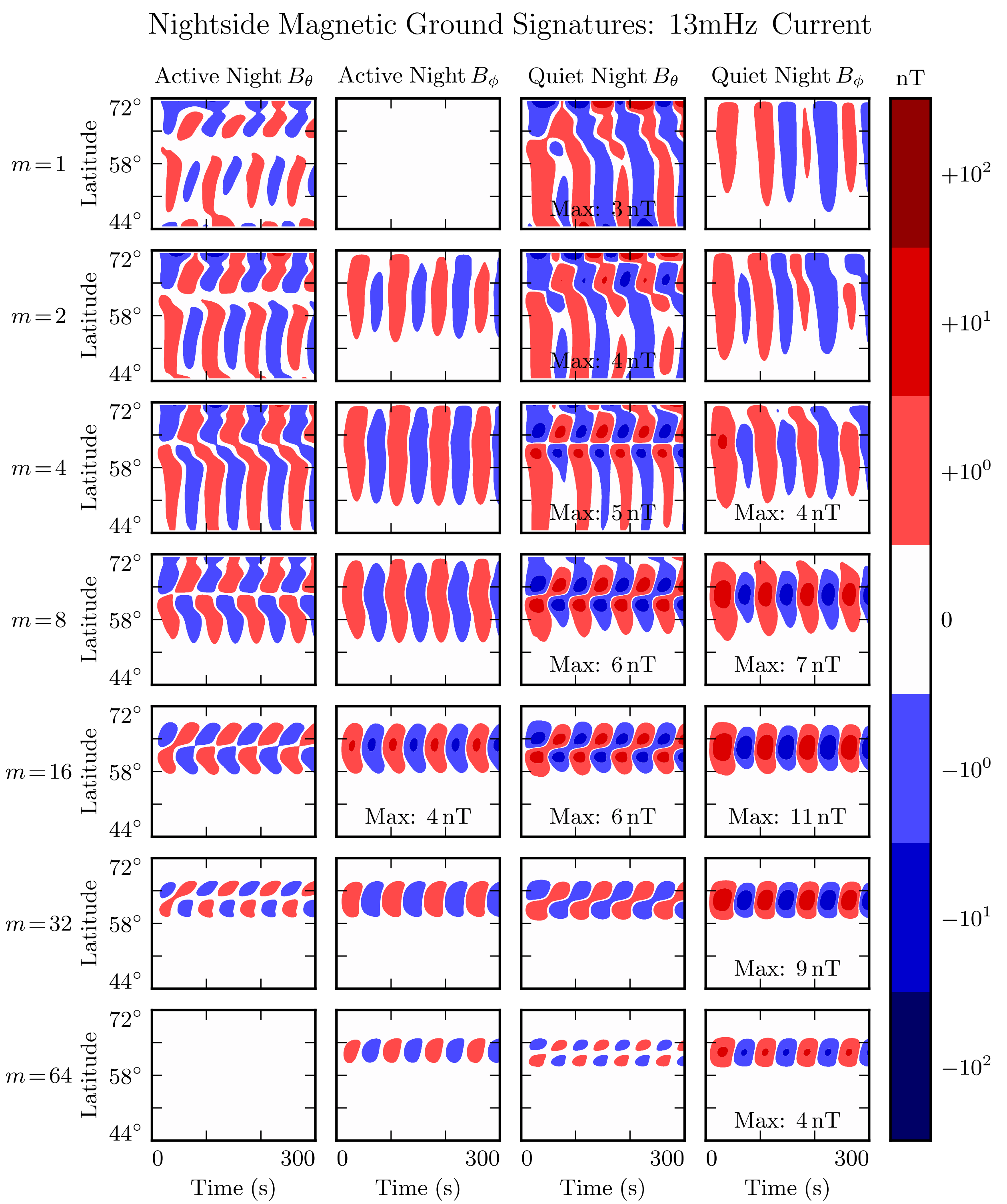

Comparison to Observations?

- How does the distribution of Pgs line up with that of odd poloidal Pc4s overall?
- Do the distributions of odd poloidal Pc4s and odd toroidal Pc4s look similar – with the toroidal ones skewed dayward?
- How about even Pc4s?

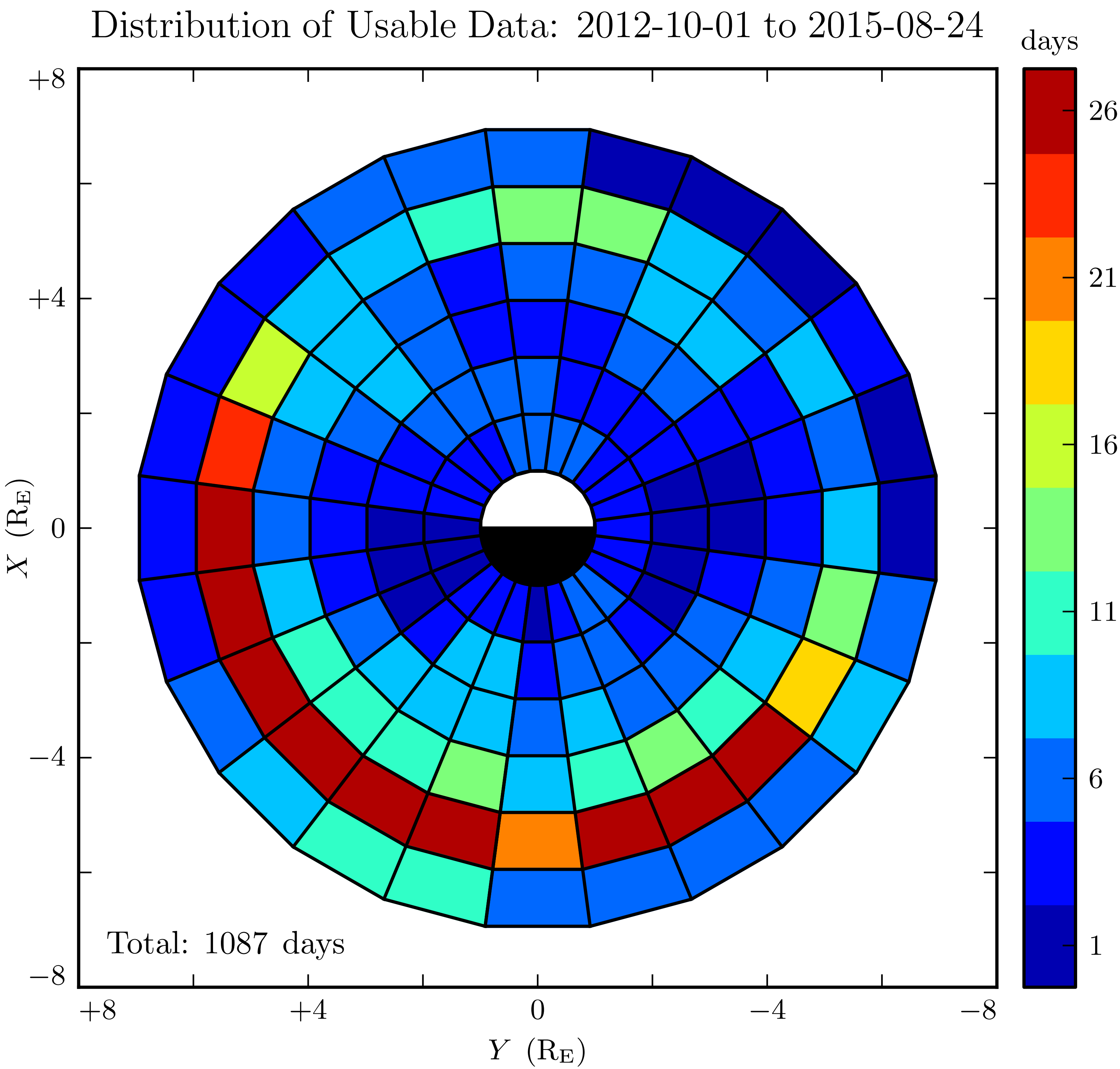

Distribution of Usable Data: 2012-10-01 to 2015-08-24
days
26
21
16
11
6
1
+8
+4
0
−4
−8
X (R_E)
Y (R_E)
Total: 1087 days

Event Selection

For each channel:

- Fit the spectrum.
- Check frequency.
- Check magnitude.
- Check coherence.
- Check parity.

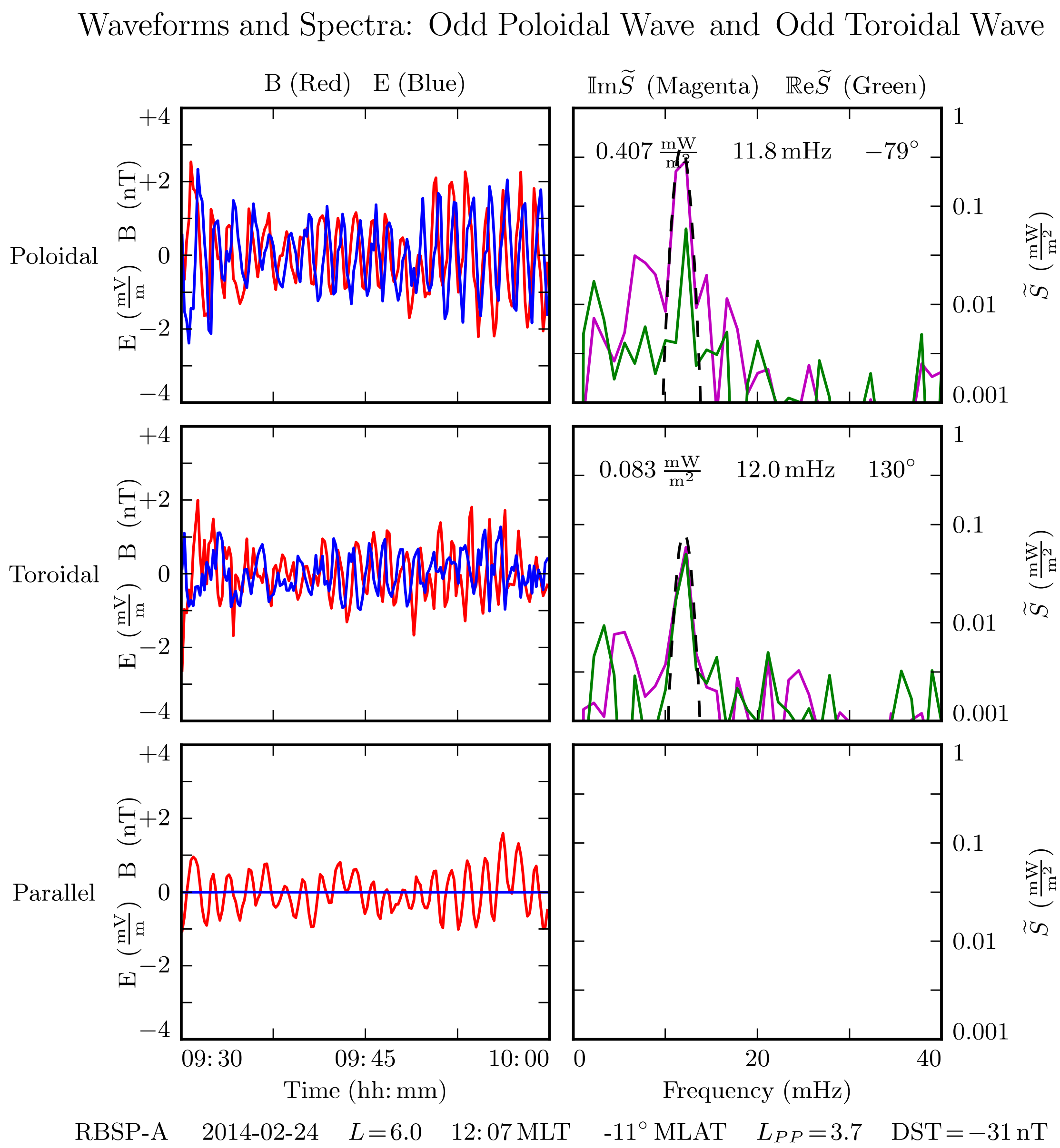

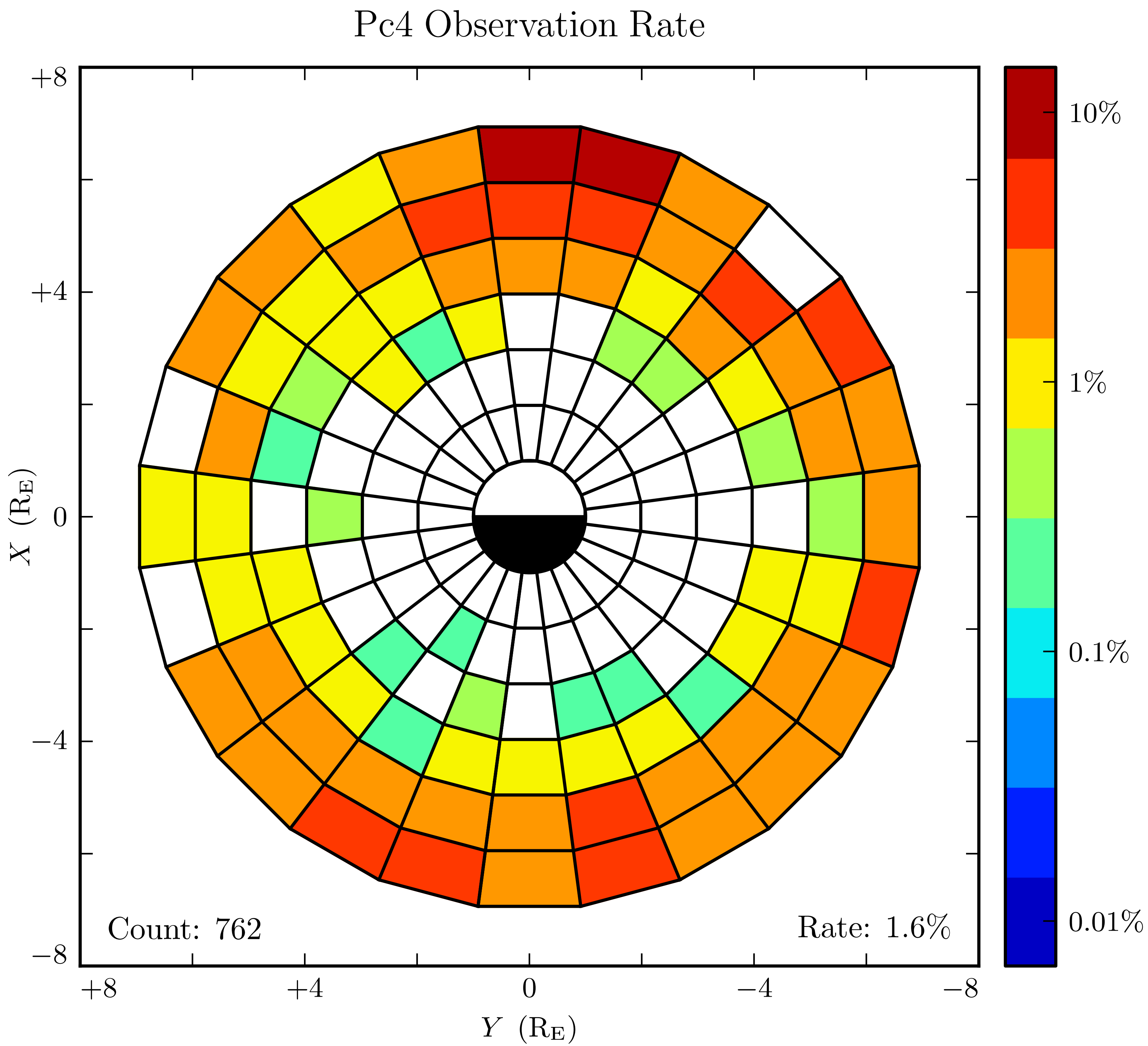

Pc4 Observation Rate
+8
+4
0
−4
−8
X (R$_E$)
Y (R$_E$)
Count: 762
Rate: 1.6%
10%
1%
0.1%
0.01%

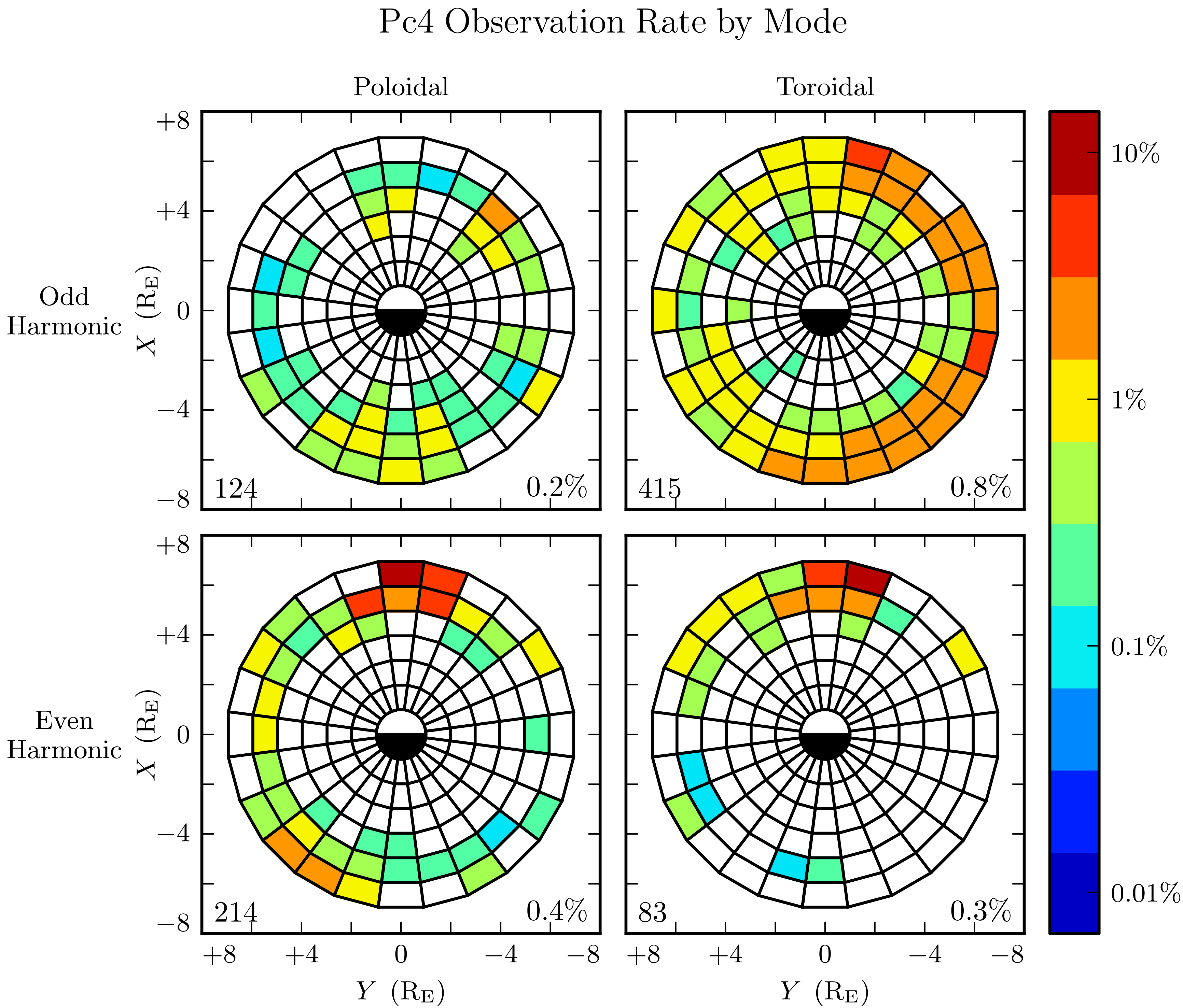

Pc4 Observation Rate by Mode
Poloidal
Toroidal
Odd Harmonic
Even Harmonic
X (R_E)
Y (R_E)
+8
+4
0
−4
−8
124
0.2%
415
0.8%
214
0.4%
83
0.3%
10%
1%
0.1%
0.01%

Summary and Conclusions

- Past work has described Pc4s in terms of a mishmash of different properties.
- Tuna is a code designed to simulate Pc4s effectively, even at high modenumber.
- Numerical results suggest novel connections between known Pc4 properties.
- In situ survey and numerical results compliment one another.